Advanced retrievals of multilayered cloud properties using multispectral measurements

Jianping Huang,[1] Patrick Minnis,[2] Bing Lin,[2] Yuhong Yi,[1] Mandana M. Khaiyer,[1] Robert F. Arduini,[3] Alice Fan,[3] and Gerald G. Mace[4]

Received 6 June 2004; revised 2 September 2004; accepted 4 October 2004; published 13 April 2005.

[1] Current satellite cloud retrievals are usually based on the assumption that all clouds consist of a homogenous single layer despite the frequent occurrence of cloud overlap. As such, cloud overlap will cause large errors in the retrievals of many cloud properties. To address this problem, a multilayered cloud retrieval system (MCRS) is developed by combining satellite visible and infrared radiances and surface microwave radiometer measurements. A two-layer cloud model was used to simulate ice-over-water cloud radiative characteristics. The radiances emanating from the combined low cloud and surface are estimated using the microwave liquid water with an assumption of effective droplet size. These radiances replace the background radiances traditionally used in single-layer cloud retrievals. The MCRS is applied to data from March through October 2000 over four Atmospheric Radiation Measurement (ARM) Southern Great Plains (SGP) sites. The results are compared to the available retrievals of ice water path (IWP) from radar data and show that the MCRS clearly produces a more accurate retrieval of ice-over-water cloud properties. MCRS yields values of IWP that are closest to those from the radar retrieval. For ice-over-water cloud systems, on average, the optical depth and IWP are reduced, from original overestimates, by approximately 30%. The March–October mean cloud effective temperatures from the MCRS are decreased by 10 ± 12 K, which translates to an average height difference of ~1.4 km. These results indicate that ice-cloud height derived from traditional single-layer retrieval is underestimated, and the midlevel ice cloud coverage is over classified. Effective ice crystal particle sizes are increased by only a few percent with the new method. This new physically based technique should be robust and directly applicable when data are available simultaneously from a satellite imager and the appropriate satellite or surface microwave sensor.

Citation: Huang, J., P. Minnis, B. Lin, Y. Yi, M. M. Khaiyer, R. F. Arduini, A. Fan, and G. G. Mace (2005), Advanced retrievals of multilayered cloud properties using multispectral measurements, *J. Geophys. Res.*, *110*, D15S18, doi:10.1029/2004JD005101.

1. Introduction

[2] Clouds, especially high clouds, are very important regulators of the hydrological and energy cycle of Earth's climate. Although the critical role of clouds in the Earth's radiation balance has been widely recognized for many years, they are still the major source of large uncertainties in climate predictions by general circulation models (GCMs). The difficulty in adequately capturing the cloud radiative effects in GCMs is well documented [*Cess et al.*, 1990]. One of the principal reasons for the large uncertainties is the poor knowledge of ice water path (IWP) distribution. Until the IWP is properly characterized by observations, it will not be possible to sufficiently constrain, for the sake of reliable climate assessment, the models' production of ice water and its subsequent effects on the hydrological and radiation budgets. Thus globally accurate IWP information is urgently needed for testing of global climate models and characterizing the radiation budget.

[3] IWP determination is often complicated because of cloud overlap. Current satellite IWP retrievals are usually based on the assumption that all clouds are single-layered, despite the relatively frequent occurrence of overlapped cloud systems. Cloud overlap can cause large errors in the retrievals of many properties including cloud height, optical depth, thermodynamic phase, and particle size. For ice-over-water clouds, one of the greatest impediments to accurately determine cloud ice mass for a given atmospheric profile is the influence of underlying liquid water clouds and precipitation on the radiances observed at the top-of-atmosphere (TOA) in the visible and near-infrared wavelengths. Although IWP can be inferred from retrievals of cloud optical depth and effective ice particle sizes using visible and infrared methods [e.g., *Minnis et al.*, 1993, 1995, 1998, 2001], it is generally overestimated when water

[1] Analytical Services and Materials, NASA Langley Research Center, Hampton, Virginia, USA.
[2] NASA Langley Research Center, Hampton, Virginia, USA.
[3] SAIC, Hampton, Virginia, USA.
[4] Department of Meteorology, University of Utah, Salt Lake City, Utah, USA.

0148-0227/05/2004JD005101$09.00

clouds are present underneath the ice clouds. The optical depth derived from the reflected visible-infrared radiances represents the combined effects of all cloud layers and the resulting IWP is actually an estimate of the total water path (TWP). When the ice-over-water cloud radiances are interpreted as if they were from an ice cloud only, the larger sizes of the ice crystals tend to yield a greater IWP (TWP) than would be expected from the simple summation of the actual IWP and liquid water path (LWP) in the column. Thus the effects of the LWP and IWP in ice-over-water cloud systems should be separated.

[4] Methods for direct retrieval of ice cloud properties using millimeter and submillimeter-wavelength measurements in all conditions [*Liu and Curry*, 1998, 1999; *Weng and Grody*, 2000; *Zhao and Weng*, 2002] are under development but have not yet been deployed on satellites. However, even for these newer techniques there are no cloud property estimates for the lower cloud layers in ice-over-water cloud systems.

[5] Currently, the most feasible approach for retrieving IWP for the overlapped cases uses a combination of microwave (MW) and visible-infrared methods. Although the visible-infrared retrievals of optical depths and effective particle sizes are for the whole column of clouds, in ice-over-water clouds, they are primarily sensitive to the upper cloud layer, especially when the upper layer ice clouds are thick. Microwave radiation, however, is mainly affected by surface, water clouds and atmospheric water vapor; it is not significantly scattered or absorbed by ice clouds. Therefore, over oceans, which have a predictable surface emissivity, it is possible to combine both visible infrared and microwave techniques to determine the presence of water clouds below the ice clouds and separately estimate IWP and LWP for each scene. *Lin and Rossow* [1996] estimated global IWP distributions over oceans by using a simple separation technique of total water path (TWP), which is assumed to be equal to the combination of LWP and IWP, retrieved from visible infrared data by the International Satellite Cloud and Climatology Project (ISCCP) and cloud liquid water path (LWP) from a microwave remote sensing method, respectively. In that case, the ISSCP and microwave data were temporally and spatially matched to no better than 1.5 hours and 30 km, respectively. A more refined microwave, visible, and infrared (MVI) technique [*Lin et al.*, 1998] was used to derive IWP in the same manner using well-matched instantaneous visible infrared scanner (VIRS) and Tropical Rainfall Measuring Mission (TRMM) Microwave Imager (TMI) data taken by TRMM over ocean [*Ho et al.*, 2003]. Those estimates mark an advance in our knowledge of global IWP but they are limited to ocean areas, are based on the simple TWP-LWP difference technique, and are difficult to validate.

[6] Over land, the variability in surface emissivity renders such an approach nearly useless. However, at several Atmospheric Radiation Measurement (ARM) Program [*Ackerman and Stokes*, 2003] surface sites, LWP is routinely derived from microwave radiometers and, at one location, cloud vertical structure is determined accurately from a combination of cloud lidar and radar data. In some cases, it is possible to simultaneously derive the IWP from the radar data even when LWP is present [*Mace et al.*, 2002]. Cloud properties have been derived every half hour for several years from visible infrared imager data taken by the Geostationary Operational Environmental Satellites (GOES) using the visible infrared solar infrared split-window technique (VISST) [see *Minnis et al.*, 2002]. Initial comparisons of the IWP retrieved from Terra Moderate Resolution Imaging Spectroradiometer data with ARM radar retrievals [*Mace et al.*, 2005] indicate that for cirrus clouds with IWP as large as 120 gm^{-2}, the mean IWP from VISST is within 5% of the radar retrieval. Instantaneous VISST retrievals are within 25% of the radar results. Those initial comparisons indicate that the satellite and radar methods yield similar results for single-layered ice clouds. By combining the GOES satellite retrievals with the surface-derived LWP over the ARM sites, it should be possible to develop a more complete IWP climatology over this limited region for single- and ice-over-water clouds and perform some validation comparisons with the surface-based IWP retrievals for ice-over-water clouds.

[7] In this paper, an improved technique is developed to estimate LWP and IWP values simultaneously using satellite and ground-based measurements over ARM Southern Great Plains (SGP) boundary and central facilities sites. Rather than simply differencing the TWP and microwave LWP in overlapped cases, this new approach performs a more explicit radiance-based retrieval of IWP to account for differences in the optical properties of ice and liquid water clouds. In overlapped cases, LWP is estimated from ARM microwave radiometer (MWR) measurements first, and then used as part of the lower boundary for a reanalysis of the satellite IWP. In the initial VISST analysis for overlapped clouds, IWP is derived assuming the entire cloud is composed of ice crystals; the surface and atmosphere together form the lower boundary condition for the retrieval. The new algorithm treats the combination of the lower cloud, the atmosphere, and the surface as the lower boundary condition. The IWP retrievals are then based on the calculation of the integrated systems of upper level ice clouds and the lower boundaries using a radiative transfer model parameterization. Preliminary validation of the retrievals is accomplished by comparisons with simultaneous retrievals using the ARM radar at the SGP central facility (SCF).

2. Satellite and Surface Data

2.1. VISST

[8] This study analyzes satellite and surface measurements taken between 1 March and 30 October 2000 over the ARM SGP domain. GOES-8 provided continuous coverage of the region and was used to derive the daytime cloud properties using the VISST, which is an upgrade of the 3-channel method described by *Minnis et al.* [1995]. VISST analyzes an array of satellite-observed visible (0.65 μm) reflectances and 3.9, 10.8, and 12.0 μm brightness temperatures at a given set of solar zenith, viewing zenith, and relative azimuth angles using a set of lookup tables in parameterizations [*Minnis et al.*, 1998] that account for the contributions of the surface and atmosphere to the radiance in each channel. Solutions are computed iteratively for both liquid and ice clouds yielding effective droplet size r_e or effective ice crystal diameter *De*, optical depth τ, and cloud radiating temperature *Tc*. Phase is determined using several criteria including the value of *Tc*, the available solution, and

the consistency of the temperature parameterized using the retrieval with the observed value. IWP or LWP is computed from the particle size and optical depth. The GOES-8 visible radiances were calibrated against VIRS as described by *Minnis et al.* [2002].

2.2. Microwave Retrievals

[9] An algorithm adapted from the satellite remote sensing method of *Lin et al.* [1998, 2001] was used to retrieve LWP and liquid water temperature (*Tw*) from the ground-based ARM SGP microwave radiometer (MWR) and infrared thermometer (IRT) measurements. The major cloud water temperature signal is from the IRT, especially when the water cloud layer is thick (optical depth >5). When the water layer is thin, the MWR-retrieved LWP is used to estimate optical depth and correct the cloud water temperature [*Lin et al.*, 2001]. Since the atmospheric water vapor measurements from the MWR are used to correct the IR brightness temperatures (*Tb*) for water vapor absorption, the accuracy of *Tw* is similar to that for the IR cloud temperature from satellite remote sensing and should be within 1–3 K, depending on the cloud LWP and optical thickness corrections. For the satellite (i.e., SSM/I or TMI) case, *Tw* is retrieved directly from high frequency (85 GHz) microwave measurements. The accuracy in the satellite case is about 8 K. The MWR has a field-of-view (FOV) of 5.9° at 23 GHz and 4.5° at 31.4 GHz. Thus the microwave estimated LWP represents the average over the microwave radiometer's FOV because of the near linear relationship between LWP and *Tb*. Although broken liquid clouds have small effects on microwave LWP retrievals, only overcast scenes are considered here to eliminate any uncertainties due to cloud inhomogeneity. The ARM MWRs measure 23.8 and 31.4 GHz brightness temperatures at 20-s sampling intervals. Retrievals of LWP from each of these samples are averaged over 30 min to obtain a mean LWP centered on the satellite observation time. The ARM ground-based MWRs are available at several locations within the SGP domain: site B1 located at 38.31°N, 97.30°W (Hillsboro, OK); B4 at 36.07°N, 99.20°W (Vici, OK); B5 at 35.69°N, 95.87°W (Morris, OK); and the SCF, C1 at 36.61°N, 97.49°W (Lamont, OK). Cloud base height information was determined using Vaisala ceilometer data at sites B1, B4 and B5 and Active Remote Sensing of Cloud Layers (ARSCL) [see *Liljegren*, 1999; *Clothiaux et al.*, 2000] data at the SCF. Surface pressure and air temperature, as well as temperature and wind direction at cloud base height, were taken from the rapid update cycle (RUC) [see *Benjamin et al.*, 2004] hourly analyses.

2.3. MVI Overlapped Cloud Selection

[10] The GOES-8 radiances and cloud properties were averaged in 0.3° boxes centered on each site and matched with half-hourly averaged MWR-retrieved cloud properties. Overcast clouds constitute about 74.2% of all of the cloudy cases. The overcast cases can be further classified as 18% ice, 38% liquid water, and 18% mixed phase based on the phase of all pixels within the box. Since the IRT provides only one temperature for the site and no information about partial cloudiness, no broken clouds are considered here. To account for the advantages of each technique, only those clouds classified as overcast ice-phase clouds by VISST are examined.

[11] The overcast ice phase clouds actually consist of single-layered ice clouds and ice-over-water cloud. The ice-over-water clouds are identified with the MVI method, which uses the difference between cloud liquid water temperature *Tw* and the effective cloud temperature *Tc*. The cloud liquid water temperature *Tw* retrieved from IRT and MWR data is close to the cloud base temperature, especially when the lower level clouds are thick [*Lin et al.*, 2001]. The effective cloud temperature *Tc* derived from GOES data represents the temperature near the top of the cloud for optically thick clouds [*Minnis et al.*, 1993]. When the difference, $\Delta Twc = Tw - Tc$, is significantly larger than zero, it is likely that the observed system consists of overlapped or mixed phase clouds [*Lin et al.*, 1998; *Ho et al.*, 2003]. In this study, the conditions required for classifying a cloud as ice-over-water for the entire 0.3° box are: 100% ice phase from VISST, $Tc < 273$ K, $Tw - Tc > 8$ K and MWR LWP (LWP_{MW}) > 10.0 gm^{-2}. If $LWP_{MW} > 750$ gm^{-2}, then the value of LWP_{MW} is reset to 750 gm^{-2}. Ice-over-water clouds were detected in 60% of the total occurrences of overcast ice clouds from all four sites. From the values of $Tw - Tc$, it was determined that most of those overlapped cloud systems consist of cold, high ice clouds over lower, warmer water clouds [*Huang et al.*, 2003].

[12] In summary, the new retrieval algorithm described in the following section is applicable to nonprecipitating systems with an ice cloud on top and a water cloud below whenever the mean temperature of the water cloud differs from that of the combined ice and water cloud infrared effective temperature by more than the separation threshold (8°K). The clouds do not have to be physically distinct layers or form in only two layers. A water cloud can be contiguous with the ice cloud as long as *Tw* and *Tc* differ by more than 8°K. For example, an altostratus under a cirrus cloud can be physically separated by a few hundred meters, but the values of *Tw* and *Tc* might be only a few degrees different. In that case, the algorithm would not detect them as multilayered. Conversely, consider three layers of water clouds below the ice cloud with the top of the uppermost water cloud touching the base of the ice cloud. In this case, *Tw* would be some value between the uppermost water cloud and the lowest water cloud resulting in a significant difference between *Tw* and *Tc*. The MVI method would detect this as a multilayered cloud and the three water cloud layers would be treated as one layer with the temperature *Tw*. Thus the new algorithm is not constrained to only two layers or to physical separation between the ice and water cloud, but is limited only by the proximity of the radiating temperatures of the ice cloud and the centroid of the water cloud masses. Further refinement of the method could be used to make it applicable to broken ice clouds over overcast water clouds, but that category is beyond the scope of this paper.

[13] To ensure that the MVI was detecting multilayered clouds properly, its selections were compared to the ARSCL data for the entire 8-month period over the SCF. The MVI missed 10% of cases that were overcast and ice-over-water overlapped. The only cases that MVI missed, however, were overcast but either the ice clouds were broken, the water clouds were scattered or broken underneath an overcast ice

cloud, or no GOES or MWR data were available. In the broken water cloud cases, the mean LWP was less than zero or the value of *Tw* was ill-defined. The broken ice cloud cases do not fall within the criteria for applying this technique and the presence of very small amounts of liquid water below the ice cloud are probably not very important as a contribution to overlapped clouds. No MVI cases were false ice-over-water detections, however, in 5% of the cases, the water and ice layers were contiguous, so technically the clouds were not overlapped, separated layers. Overall, it is concluded that this is an excellent method for detecting ice-over-water clouds.

3. Development of Multilayered Cloud Retrieval System (MCRS)

[14] In the MVI method, it is assumed that, for overcast multilayered ice-over-water clouds, the VISST-derived IWP equals TWP. Therefore the "true" ice water is estimated by the MVI technique through simple differencing as

$$\mathrm{IWP} = \mathrm{TWP} - \mathrm{LWP}, \tag{1}$$

where LWP is from the MWR retrieval. In reality, the microphysical properties of the low-level clouds significantly influence the VISST-derived optical depths and effective diameters subjecting the simple differencing method to potentially large biases. To illustrate this point, adding-doubling radiative transfer calculations of visible reflectance were performed using the microphysical model, T40 (*De* = 67.6 μm; see *Minnis et al.* [1998]) for an ice cloud at a temperature of −40°C for various optical depths as a single-layered cloud and as part of a two-layered cloud system. In the latter case, the lower layer was assumed to be a water cloud with effective droplet radii, *re* = 8 μm (r8) and 12 μm (r12), and LWP = 100 gm^{-2}. The visible reflectance was computed for both the single and multilayered clouds for TWP up to 600 gm^{-2}. Examples of the results are plotted in Figure 1 for two solar zenith θ_o, one viewing zenith θ(45°), and three relative azimuth φ angles. In the top panel, the reflectance (thin curve) for $\theta_o = 60°$, $\phi = 25°$ and T40 increases from 0.52 at TWP = 100 gm^{-2} to 0.66 for TWP = 200 gm^{-2} up to 0.84 for TWP = 600 gm^{-2}. The reflectance (thick curve) for T40 at $\theta_o = 30°$ starts at a lower value and follows a similar curve. If lower-level clouds exist, the reflectances are greater than those of single layer clouds for a given TWP. For example, when TWP is around 100 gm^{-2} (LWP = 100 gm^{-2}, IWP ∼ 0), T40/r12, and θ_o = 60°, the reflectance is 0.65, while the single-layer ice clouds with the same amount of TWP would produce a reflectance of 0.52. This effect causes current satellite retrievals to overestimate IWP or TWP when the lower cloud is present. An assumed cloud with both IWP and LWP equal to 100 gm^{-2} (TWP = 200 gm^{-2}) would have a reflectance 0.73. The current VISST retrieval would assume that the entire cloud consists of ice particles, and then, following the T40 curve, obtain IWP = TWP = 300 gm^{-2}. If a microwave retrieval of LWP = 100 gm^{-2} is used to estimate IWP, the MVI method would yield 200 gm^{-2} instead of 100 gm^{-2}. The error is even worse for the T40/r8 case. While the forward scattering direction (φ = 25°) represents an extreme case, most of the other results (seen in the lower panels of Figure 1)

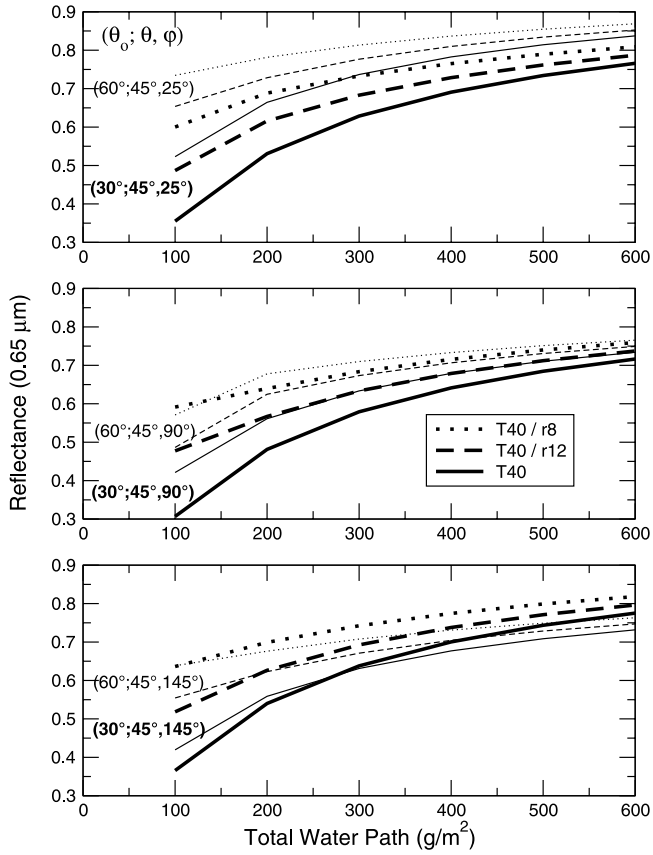

Figure 1. Reflectance at 0.65 μm as a function of total cloud water path from adding-doubling RTM calculations for six sets of viewing and illumination conditions. The solid curves are for a single-layer ice cloud (T40 model with *De* = 67 μm) and the broken curves are for a T40 ice cloud over a water cloud with LWP = 100 gm^{-2}. Results are shown for *re* = 8 and 12 μm. In each panel the thick solid and broken curves represent results with a smaller viewing zenith angle (30°), and the thin ones are for a larger viewing zenith angle (60°).

would yield overestimates of IWP using the MVI approach. Since the operational VISST uses τ and *De* as its retrieval products, and water cloud droplets are much smaller (a factor of 2–3) than ice crystals, most of the overestimation discussed above is compensated through underestimation of column total optical depths and overestimation of averaged column effective particle sizes. Nevertheless, there are significant errors inherent in the MVI algorithm that will depend on the viewing and illumination angles and relative amounts of ice and water.

[15] To improve the accuracy of ice cloud property retrievals, a new retrieval algorithm is developed for multilayered cloud system. A schematic view of this new algorithm, the multilayered cloud retrieval system (MCRS), is outlined in Figure 2. Initially, the VISST retrieval is performed using the surface as the background and the MWR retrieval is used to derive LWP and *Tw*. The results are used in the MVI method to detect the cloud overlapping by using the difference between the value of cloud water temperature *Tw* retrieved from IRT data and the cloud effective temperature *Tc* derived from satellites. When the

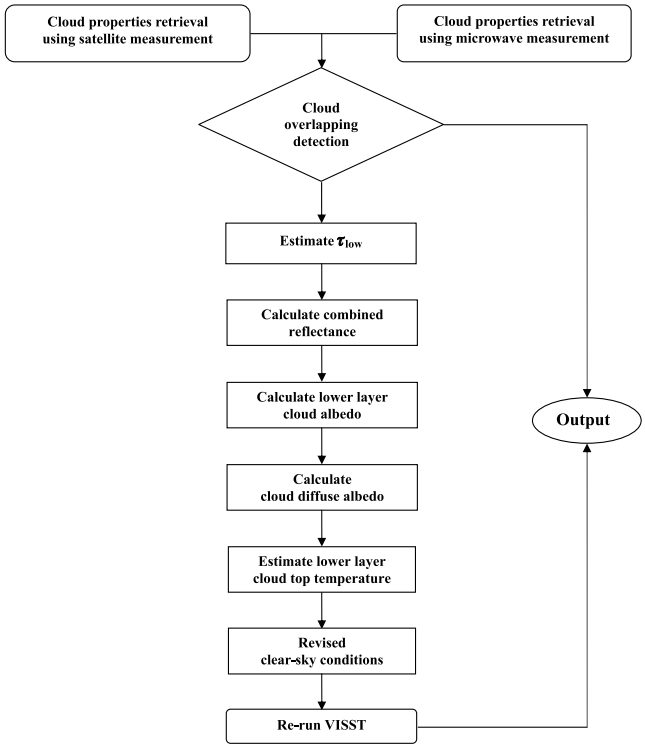

Figure 2. Schematic view of the multilayered cloud retrieval system (MCRS).

difference, $\Delta Twc = Tw - Tc$, is significantly positive, it is likely that the observed system consists of overlapped clouds as discussed in the previous section and in the work of *Lin et al.* [1998], *Ho et al.* [2003], and *Huang et al.* [2003].

[16] Second, the optical depth of the low-level water cloud is estimated as

$$\tau_{low} = 0.75\ Q_{vis}(r_e)\mathrm{LWP_{MW}}/r_e. \quad (2)$$

where $Q_{vis}(r_e)$ is the extinction efficiency at a given effective droplet radius. In this study, r_e is assumed to be 8 μm. This effective water cloud particle size is very close to the statistical mean values obtained from single layer water clouds over the ARM site [e.g., *Dong et al.*, 2000]. The value of $\mathrm{LWP_{MW}}$ is from the MWR retrieval.

[17] In the third step, the combined reflectance is calculated by first computing the direct and diffuse reflectance at 0.65 μm for the combined surface, low water cloud, and atmosphere below the low water cloud to serve as the background reflectance field for a second VISST retrieval. Similarly, the value of *Tw* is adjusted to replace the surface skin temperature used in the initial retrieval and serves to provide the background emitted radiances at 3.9, 10.8, and 12.0 μm. Since cloud liquid water temperature *Tw* retrieved from IRT and MWR data is close to cloud base temperature, especially when the lower level clouds are thick [*Lin et al.*, 2001], the water cloud top temperature is given by

$$T_{wc} = T_w - g\Delta Z/R \quad (3)$$

where g and R are the constant; ΔZ is water cloud thickness which is estimated by

$$\Delta Z = 0.085\tau_{low}^{1/2},$$

as given by *Minnis et al.* [1995]. The resulting VISST retrieval, therefore, accounts for the changes in the reflectance field due to the upper layer cloud only. The low cloud-surface-lower atmosphere reflectance field is computed using the lookup tables of *Minnis et al.* [1998] in the parameterization reported by *Arduini et al.* [2002]. The new ice cloud top temperature T_c is computed using the cloud emissivity and the observed 10.8-μm brightness temperature *T*. For optically thin water clouds, the ice cloud top temperature is estimated from the observed radiance:

$$B(T) = (1-\varepsilon_c)(1-\varepsilon_w)\varepsilon_s B(T_s) + (1-\varepsilon_c)\varepsilon_w B(T_{wc}) + \varepsilon_c B(T_c) \quad (4)$$

where ε_s, ε_c and ε_w are the surface, upper layer ice cloud and lower-layer water cloud emissivities at 10.8 μm, respectively, and B is the Plank function evaluated at 10.8 μm. The values of ε_c and ε_w are estimated as

$$\varepsilon_c = 1 - \exp\left[a(\tau_c/\mu)^b\right] \quad (5a)$$

and

$$\varepsilon_w = 1 - \exp\left[a(\tau_{low}/\mu)^b\right], \quad (5b)$$

respectively. The coefficients a and b depend on cloud microphysics [see *Minnis et al.*, 1993]. *Ts* is surface skin temperature. When τ_{low} is large (i.e., $\varepsilon_w = 1$), equation (4) can be simplified as

$$B(T) = (1-\varepsilon_c)B(T_{wc}) + \varepsilon_c B(T_c) \quad (6)$$

The new ice cloud properties, such as *Tc*, τ and *De* from the second VISST retrieval are then used to calculate a new value of IWP. The only assumed microphysical parameter then is the effective droplet radius of the low-level cloud.

4. Case Studies

[18] The application of the MCRS and the resulting changes in the ice cloud properties are best illustrated using a combination of surface-based passive and active sensors at the SCF. Figure 3 shows examples of cloud radar reflectivity signals of multilayered clouds over the SCF during 3 days in 2000. The radar signals were obtained from the millimeter wave cloud radar (MMCR) system located at the SCF. The zenith-pointing MMCR system operates at 35 GHz and can probe the extent and composition of most clouds. These times were selected because the multilayering conditions met the criteria for retrieving the ice cloud properties using the method of *Mace et al.* [2002]. As indicated in Table 1, these cases cover a wide range of viewing, illumination, and scattering angles. The value of θ is constant at 47.64°. For this initial VISST retrieval, the value of TWP is equal to the IWP. As shown in Figure 3,

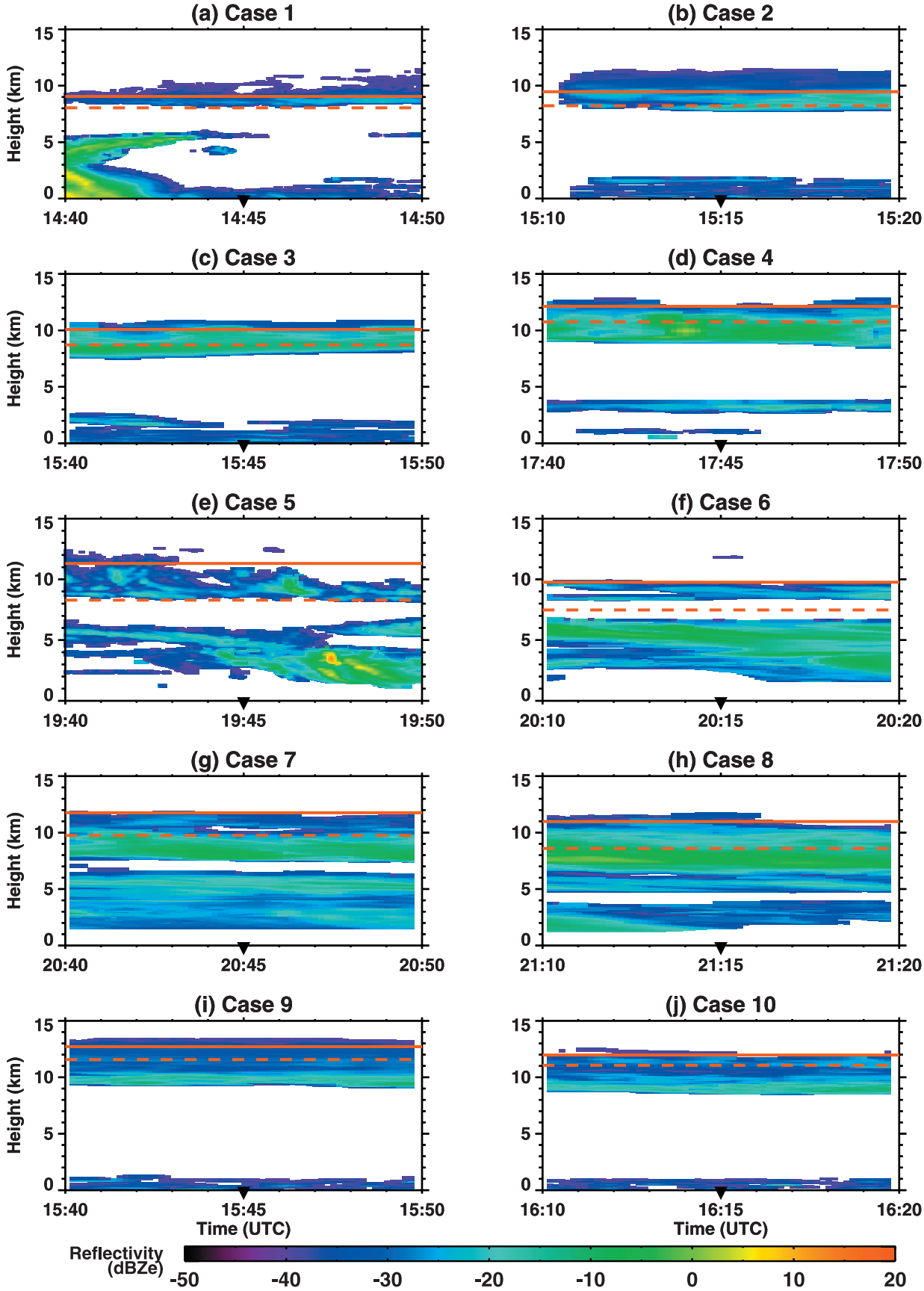

Figure 3. Millimeter wave cloud radar (MMCR) reflectivity observed at ARM SGP central facility site for ten multilayered cloud cases. The solid red and dashed lines represent the cloud height derived from MCRS and VISST, respectively.

Table 1. Viewing, Illumination, and Scattering Angles for GOES-8 and the Surface at the SCF During 2000

Case	Date	Time, UTC	θ_O, deg	ϕ, deg	Scattering Angle, deg
1	22 March	1445	64.21	144.53	146.92
2	22 March	1515	58.66	150.27	154.21
3	22 March	1545	53.38	156.70	161.34
4	27 June	1745	16.88	173.54	148.00
5	27 June	1945	20.43	90.92	128.56
6	27 June	2015	25.65	79.37	122.37
7	27 June	2045	31.31	71.10	115.98
8	27 June	2152	37.18	64.67	109.41
9	3 July	1545	38.84	133.38	146.92
10	3 July	1615	32.95	139.53	149.88

the vertical structure of the multilayered cloud is complex. For example, in Figure 3d, a high (~10.5 km), cold (232.0 K) and thick ice cloud overlaps a low (~3 km), warm (284.8 K) and thin water cloud. The initial value of *Tc* from the VISST is about 53°C less than *Tw*, which translates to a height difference of ~7.5 km. The ice cloud thins out and splits in Figures 3e–3f while the water layer thickens and is joined by another one. In Figure 3f, the ice cloud effective height and temperature from VISST are ~7.5 km and 255 K, respectively, and the MWR cloud water temperature is 287 K. The retrieved ice cloud height is clearly less than the real upper layer cirrus altitude. The LWP is ~61 gm^{-2}, which is almost double the value in Figure 3d. Figures 3g–3h also represent thick ice-over-water cloud cases except the lower layers are generally thicker than that in Figure 3c. A more complex case is seen in Figure 3a, where the lower-level clouds may be double-layered with a broken layer at bottom. Simpler cases are seen in Figures 3b, 3i, and 3j.

[19] Figure 4 compares the estimates of τ, *De*, and *Tc* derived from the MCRS with those from the initial VISST for the cases in Figure 3. For all cases, the MCRS reduced the originally overestimated ice cloud optical depth (Figure 4a) and temperature (Figure 4c) while it increased the ice crystal effective diameter (Figure 4b). As expected, the reduction in τ is most significant for the cases with thin cirrus over thick water clouds. The retrieved optical depth, for instance, decreases from 11.72 to 6.75 for case 3, from 12.0 to 3.89 for case 6, and from 13.62 to 4.5 for case 7. The average optical depth is reduced by more than 100% for the three cases. For thick-ice-over-thin-water clouds, the estimated changes in τ are around 20–40%. For example, τ decreases from 11 to 7 for case 4 and 6 to 5 for case 9. The relative change in *De* for the new algorithm is not as dramatic as that in optical depth. For case 7, *De* increased from 71.5 to 90 μm and from 58.29 to 64.52 μm for case 8. When the upper layer cloud becomes optically thick, say $\tau > 6$ or 8, the lower cloud has minimal effect on the retrieved value of *De* because a negligible amount of 3.9-μm radiation from the lower cloud passes through the upper cloud to be received by the satellite. This effect is especially evident for cases 1–4 when the water cloud is thin. The derived ice cloud temperatures decreased from 7 to 22 K (Figure 4c) with corresponding improvements in the cloud heights (see solid lines in Figure 3).

[20] Figure 5 shows a comparison of IWP derived from the MCRS with the values from the VISST and the MVI (see equation (1)), and from the MMCR using an algorithm that combines measurements of Doppler velocity with radar reflectivity [*Mace et al.*, 2002]. The new MCRS algorithm produces smaller values than the VISST for all cases and the MVI for most cases. In all of the cases, except case 5, the MCRS yields values of IWP that are closest to those from the radar retrieval. The differences are greatest for case 7 when IWP (in MCRS) is around 200 gm^{-2} less than the

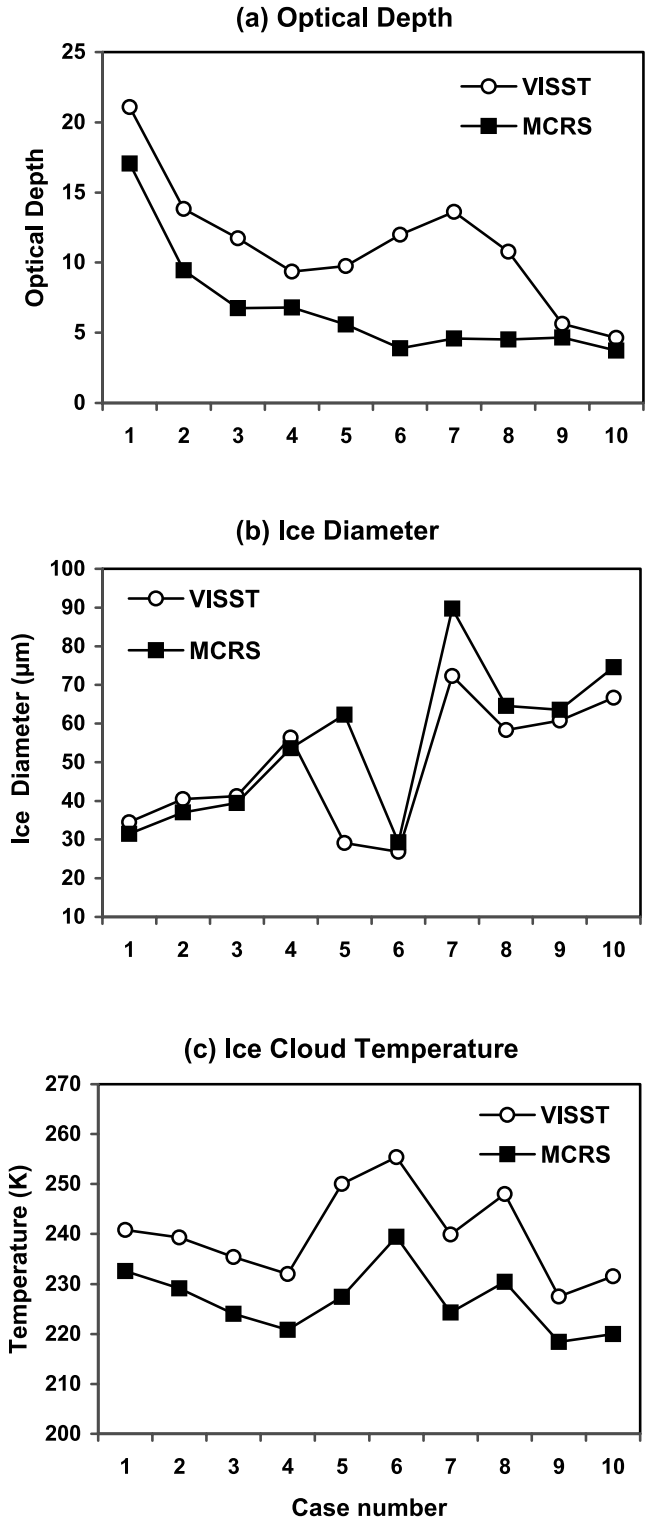

Figure 4. Comparison of ice cloud properties derived from MCRS and VISST for the 10 cases shown in Figure 3.

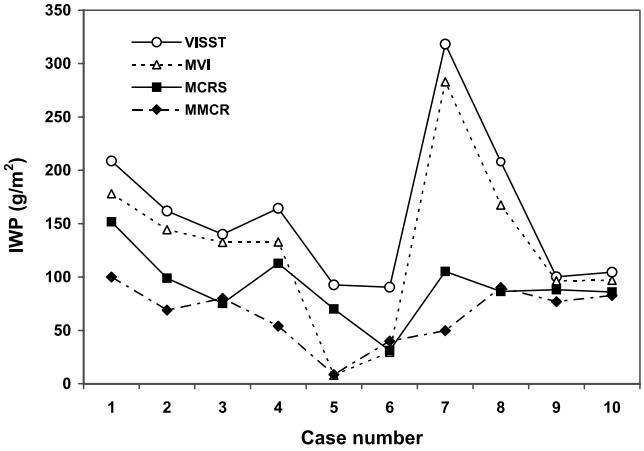

Figure 5. Comparison of ice water path (IWP) derived from the MCRS, VISST, MVI differencing (TWP-LWP), and millimeter wave cloud radar (MMCR) reflectivity for the 10 cases shown in Figure 3.

other two satellite retrievals. Both the MCRS and MVI results agree well with the MMCR data for case 6, while the MVI is closest to the radar retrieval for case 5. On average, for these cases, the difference between the MCRS and MMCR IWPs is 27 gm^{-2}, which is 37% of the mean MMCR value of 65 gm^{-2}. The difference is less than half that between the MVI and MMCR and almost 3.5 times smaller than the mean VISST-MMCR difference. Thus it is clear for these results that the MCRS represents a marked improvement over both the MVI and the single-layer VISST retrieval. In both of the earlier algorithms, the TWP is the same. The MCRS reduces the TWP, on average, because it generates a new value of IWP. The improvement in IWP is consistent with the improvement in the cloud top altitudes (Figure 3).

[21] The accuracy of the MMCR retrieval is generally on the order of ±50% and requires that the ice portion of the cloud layers is properly identified. For some of the cases in Figure 3, determining the exact boundaries of the ice cloud could result in biases in the MMCR retrieval. Validation of MCRS using the MMCR retrieval is difficult because the MMCR retrieval, in its present state, does not account for attenuation of radar energy in liquid clouds, therefore it is generally applicable only when the LWP is relatively small and no precipitating clouds are present. Therefore very few validation cases were found over the SGP for the period considered here.

5. Results and Discussion

[22] To assess how the MCRS changes the IWP in the multilayered overcast cases overall, it is necessary to examine all of the results from the four sites over the 8-month period. Figure 6 compares the ice cloud properties derived using the MCRS (black bar) with the VISST (gray bar) for ice-over-water cloud systems. The major differences between the two methods are evident in the optical depth frequency distributions (Figure 6a). The optical depths derived from the MCRS are significantly shifted to smaller values. Cloudy pixels with $\tau < 8$ comprise more than 30% of the data compared to only 9% for the VISST retrievals. The 8-month mean optical depth drops to 29.7 from 38.6. The mean relative change in τ is around 30.5% given that the relative change is defined as

$$R_c(X_{MCRS}) = \frac{(X_{VISST} - X_{MCRS})}{X_{VISST}} * 100\%, \quad (7)$$

where X_{VISST} and X_{MCRS} are the cloud properties derived from VISST and MCRS, respectively. For *De*, the March–October mean from this study (Figure 6b) is 64.9 μm, which is 1.3 μm greater than the original VISST average *De*. The averaged relative change is ~3.8%. As expected, the ice

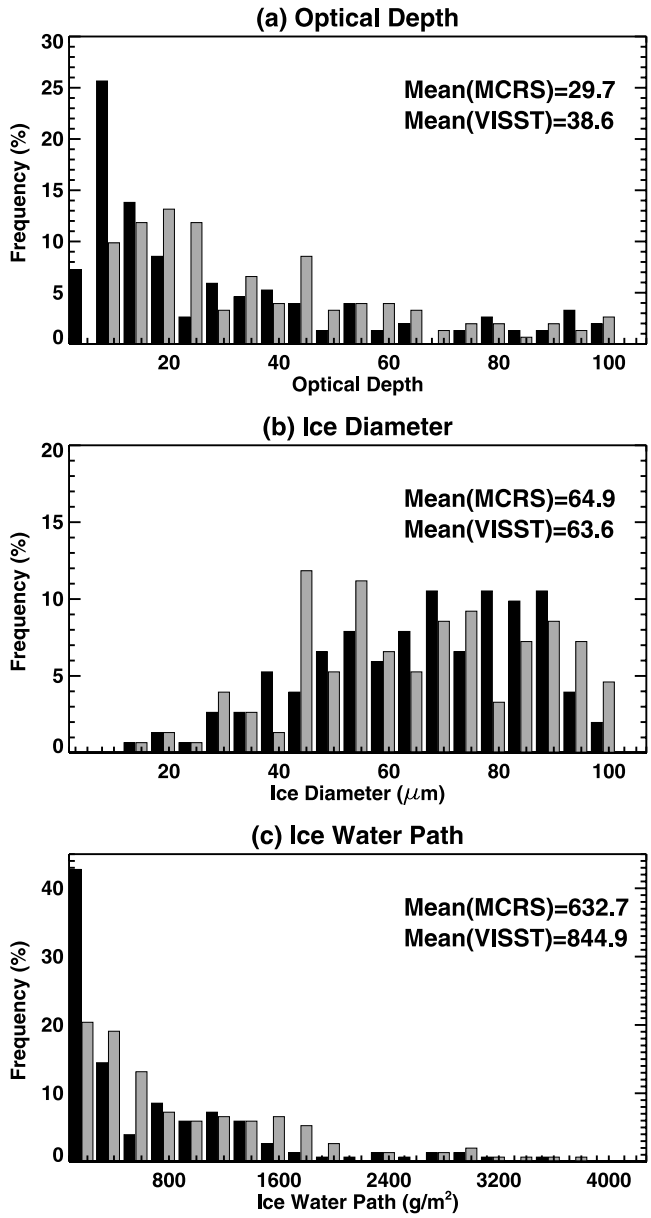

Figure 6. Comparison of ice cloud properties derived from MCRS (black bar) with VISST (gray bar) for (a) optical depth, (b) ice diameter, and (c) ice water path for ice-over-water clouds over four ARM SGP sites (March–October 2000). The histogram intervals are 5 for (Figure 6a), 5 μm for (Figure 6b), and 200 gm^{-2} for (Figure 6c).

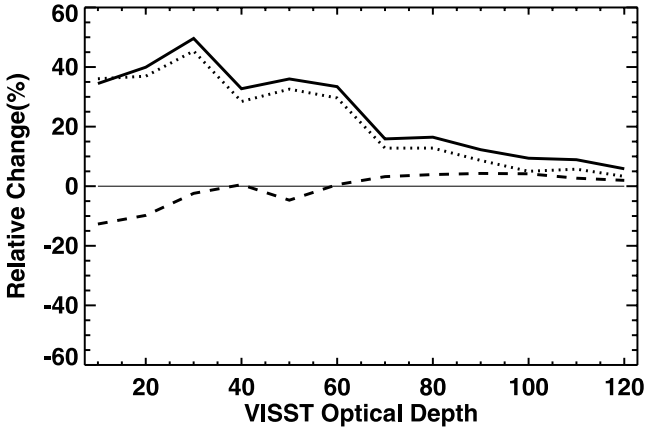

Figure 7. Changes in ice cloud properties derived from MCRS relative to the properties derived from VISST as a function of VISST optical depth for ice-over-water clouds over four ARM SGP sites (March–October 2000). Solid line is for IWP, dotted line for optical depth, and dashed line for ice diameter.

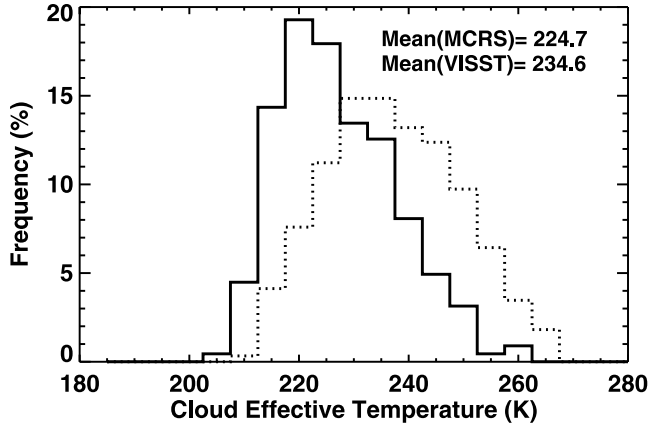

Figure 8. Comparison of cloud effective temperature derived from MCRS (solid line) and VISST (dashed line) for ice-over-water cloud systems over four ARM SGP sites (March–October 2000). The histogram interval is 5 K.

water path (IWP) values derived from the current algorithm (Figure 6c) are considerably smaller than those derived from VISST; the March–October mean IWP decreases from 844.9 gm^{-2} to 632.7 gm^{-2}. For the MCRS retrievals, clouds with IWP < 200 gm^{-2} account for around 40% of the total compared to only 20% of those from VISST. The mean relative change is 33.7%, which is only slightly larger than $R_c(\tau)$ but much larger than that for the ice diameter.

[23] *Minnis et al.* [1998] estimate ice water path from the directly derived properties as

$$IWP = \tau\left(a_1 D_e + a_2 D_e^2 + a_3 D_e^3\right), \tag{8}$$

where a_i are regression coefficients. Using (8), it can be shown that R_c(IWP) is linearly related to $R_c(\tau)$ and nonlinearly related to $R_c(De)$. However, the dependence of R_c(IWP) on $R_c(\tau)$ is only slightly greater than its variation with $R_c(De)$.

[24] Figure 7 shows R_c for the three ice cloud properties as a function of VISST optical depth (τ_{VISST}) for ice-over-water clouds. The τ_{VISST} derived from the reflected visible radiance represents the combined effects of all cloud layers. As such, cloud overlap causes large errors in the retrievals of ice cloud optical depth, ice water path, and particle size. For more than 75% of the overcast overlapping clouds ($\tau_{VISST} \leq 60$, also see Figure 6a), the MCRS reduces the ice cloud optical depth and IWP by more than 30%. The relative change for larger optical depths is generally smaller suggesting that in those cases, the ice cloud contains most of the mass in the multilayered systems. The maximum R_c for IWP and τ, ~45%, occurs at $\tau_{VISST} = 35$. However, for multilayered clouds with $\tau_{VISST} > 60$, R_c for τ and IWP decreases with the increasing of τ_{VISST}. For thin overlapped clouds ($\tau_{VISST} \leq 10$), the results from the new algorithm indicate that *De* is underestimated by 15% (i.e., $R_c(De) \sim -15\%$), but $R_c(De)$ becomes very small when τ_{VISST} exceeds 10. Given that $R_c(\tau)$ averages about 30% or less for $\tau_{VISST} > 10$, it is evident that the ice clouds are generally optically thick and, therefore, the initial VISST retrieval yields a relatively accurate value of *De*. On average, relative to the VISST, the MCRS reduces τ and IWP by 8.9 (23%) and 212.1 gm^{-2} (25%), respectively, and increases *De* by 1.3 μm (2%).

[25] Figure 8 compares the histogram of upper layer cloud effective temperature derived from new algorithm (solid line) and VISST (dash line). The temperatures from the new algorithms are decreased by 10 ± 12 K, on average, which translates to a height difference of ~1.4 km. The results in Figures 3 and 8 indicate that ice-cloud height derived from the traditional single-layer satellite retrieval is underestimated and over classifies midlevel ice cloud coverage.

[26] Figure 9 shows the histogram of IWP derived from the MCRS (black bar) and the MVI method (gray bar) for ice-over-water cloud systems. The major difference between the MCRS and MVI methods is that MVI method yields about 11% negative IWP values while there are no negative values with the new algorithm. The MVI negative IWP

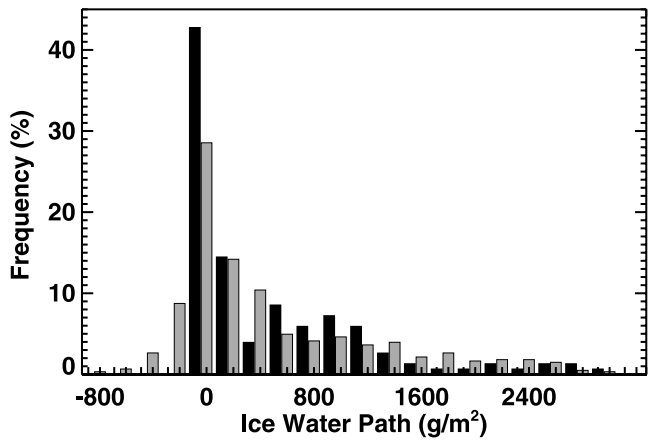

Figure 9. Comparison of ice water path derived from MCRS (black bar) and MVI (gray bar) for ice-over-water cloud systems over four ARM SGP sites (March–October 2000). The histogram interval is 200 gm^{-2}. The 0–200 gm^{-2} range bin is represented by 0.

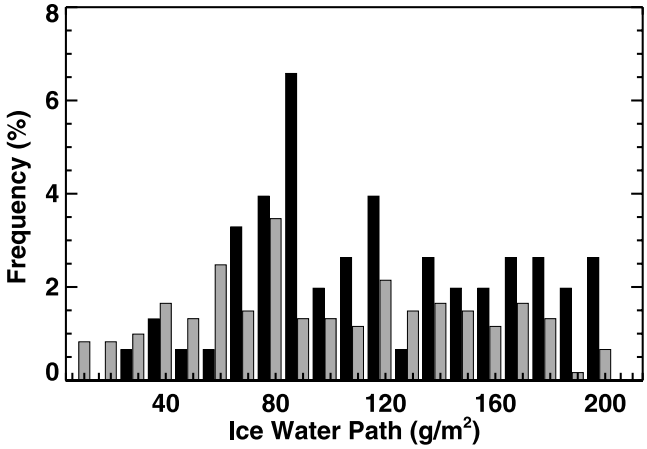

Figure 10. Detailed view of the 0–200 gm^{-2} histogram bin in Figure 9 using 10 gm^{-2} bins.

values are physically meaningless and are obtained mainly due to the uncertainties in the large LWP of the lower-level water clouds, the errors in the retrieved TWP when ice phase is assumed for whole column cloud particles, and the small signal of thin upper layer ice clouds. Another difference between these two methods is that 42% of the MCRS retrievals have IWP $\leq$ 200 gm^{-2}, while the MVI retrievals yield only 28% pixels with IWP in the same range. The 14% difference is due to the negative IWP values from the MVI method. For IWP > 200 gm^{-2}, the frequency distribution of the current algorithm agrees well with the MVI method. Figure 10 compares the detailed histogram distribution of IWP for the 0–200 gm^{-2} range with bin sizes of 10 gm^{-2}. For the 0–50 gm^{-2} range, the MCRS has only 2.6% of total while the MVI yields 5.3% with IWP values in the range of 0–50 gm^{-2}. However, the new algorithm produces more than 36.6% of its retrievals in the range of 51–200 gm^{-2}, while the MVI only has 22.3% in the same range. Figures 9 and 10 suggest that the MCRS can significantly improve, not only the retrieval accuracy, but also the physical meaning of the ice cloud properties in multilayered cloud systems. The MCRS is also expected to diminish the overestimations of τ and IWP and to increase the underestimated *De* in these same cases.

[27] Figure 11 shows *Rc* for the ice cloud properties as functions of LWP_{MW}. For the overlapped cloud with 100 gm^{-2} < LWP_{MW} $\leq$ 400 gm^{-2}, *Rc* is very stable with values around 20%–35% for both optical depth and IWP, and −3% for ice diameter. For overlapped clouds with LWP_{MW} $\leq$ 100 gm^{-2}, the *Rc* values are considerably smaller than for those overlapped clouds with LWP_{MW} > 100 gm^{-2} and they increase with increasing LWP_{MW}. This behavior is not surprising because uncertainties in the thin water-cloud LWP should not cause a large retrieval error for VISST. For overlapped cloud with LWP_{MW} > 400 gm^{-2}, *Rc* changes very rapidly with increasing LWP_{MW}. It suggests that, when lower-layer water clouds are drizzling or contain large droplets, both the microwave technique and the MCRS may have significant errors as a result of the precipitation-sized hydrometeors.

[28] Figure 12 shows the sensitivity of the new algorithm to the assumption of the droplet size in lower layer cloud. It suggests that the retrieved properties are not sensitive to the assumed droplet size. When r_e changes from 6 to 8 μm (33% increase), the mean optical depth and IWP increase by only 5.8% and 5.5%, respectively. Thus the differences between the MCRS and radar IWP values in Figure 5 are not likely due to the droplet size assumption. For thin-ice-over-thin-water cloud cases, the estimated ice cloud properties may be affected by this assumption. For the lowest category of optical depth (τ < 5) in the figure, for instance, the frequency drops by more than 5% when r_e changes from 8 to 10 μm. There is almost no change for the thicker ice cloud systems.

[29] Similarly, Figure 13 summarizes the sensitivity of the ice cloud properties to the uncertainty in LWP (±40 gm^{-2}) from the MWR retrieval. Overall, the ice cloud properties are more sensitive to an underestimate of LWP than to an overestimate. The optical depth increases by ~10% for a 40 gm^{-2} underestimate in LWP compared to only 2% for an excess LWP of 40 gm^{-2}. The ice crystal size is only affected by ±2%, while the uncertainty in the LWP translates to an uncertainty of −7.6% to 3% in IWP. The sensitivity is larger for smaller values of IWP. The MCRS was also used to test the sensitivity of the retrieval tests to the ±15% uncertainty in LWP derived from MWR. The IWP RMS errors for LWP − 15% and LWP + 15% are 53.76 gm^{-2} and 52.48 gm^{-2}, respectively.

6. Conclusion

[30] A more rigorous multilayered cloud retrieval system has been developed to improve the determination of high cloud properties in multilayered clouds. The MCRS uses a more realistic interpretation of the radiance field than earlier methods because it explicitly resolves the radiative transfer that would produce the observed radiances. A two-layer cloud model was used to simulate multilayered cloud radiative characteristics. It uses a simplified visible reflectance parameterization that could produce some uncertainties that will be examined in future studies. Surely, use of explicit two-level radiative transfer calculations could reduce the uncertainties in the retrievals. Despite the use of a simplified two-layer cloud reflectance parameterization, the MCRS clearly produced a more accurate retrieval of ice water path than the simple differencing techniques used in

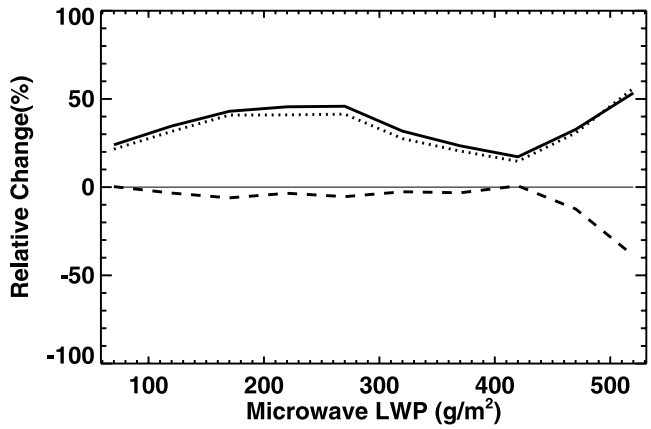

Figure 11. Same as Figure 7, but as a function of microwave LWP of lower-level water cloud.

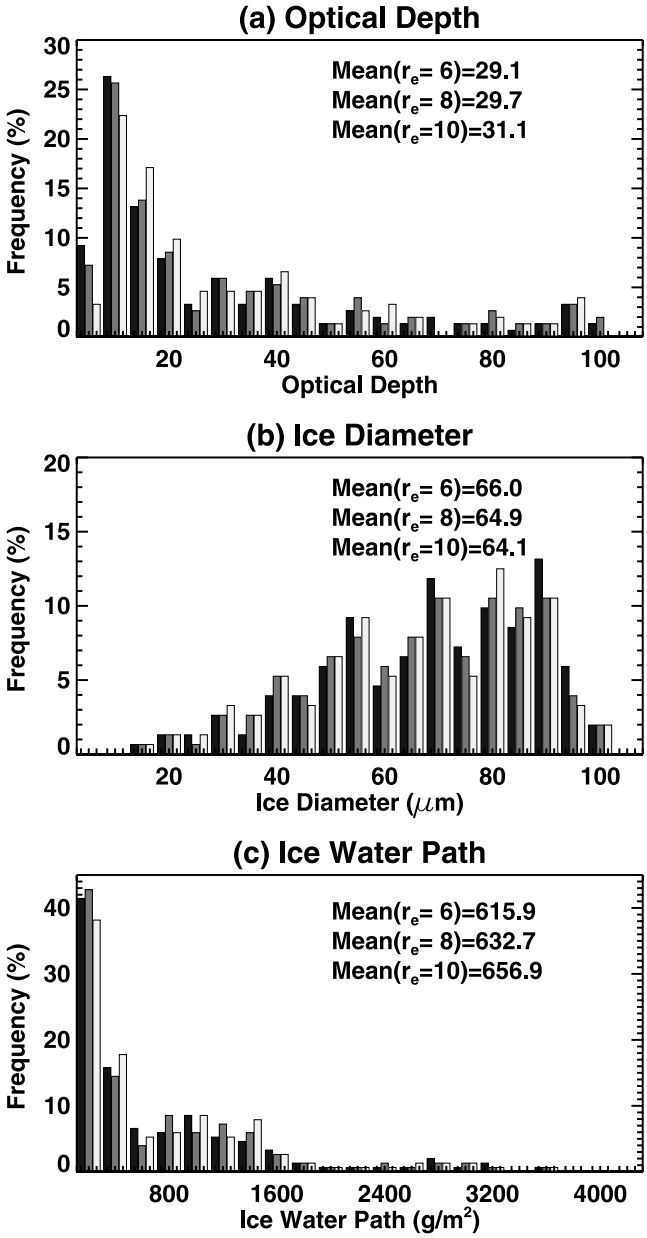

Figure 12. MCRS sensitivity to lower-layer water cloud droplet size assumption for ice-over-water cloud over four ARM SGP sites (March–October 2000): *re* = 6 μm (black bar), 8 μm (gray bar), and 10 μm (light gray bar).

the past. The initial results indicate that it still might overestimate IWP for overlapped cases, but by much smaller amounts than other techniques. However, many more comparisons with radar-MWR retrievals are required and a better assessment of the errors in the radar retrievals is needed. The method is not particularly sensitive to the assumed droplet size or the uncertainties in the MWR retrievals. The errors are smaller than the differences between the radar and MCRS retrievals. Thus this new physically based technique should be robust and directly applicable when the appropriate microwave and satellite imager data are available.

[31] Such data are available from a variety of satellites and should be exploited to derive the ice cloud properties over ocean where the LWP can be derived reliably. Over land, the variability in surface emissivity renders the microwave approach nearly useless. Thus surface radiometers like those at the ARM sites are the only source for applying this technique. With further validation against the radar retrievals and perhaps aircraft in situ data, the method could be used as reference source for other techniques that are available or being developed using other combinations of spectral radiances. Because it does not require the presence of cloud radar, only the microwave radiometer, this method could be applied at any location having the microwave radiometer providing the opportunities for validating other methods in many more conditions than possible using the radar retrievals. In the short term, this

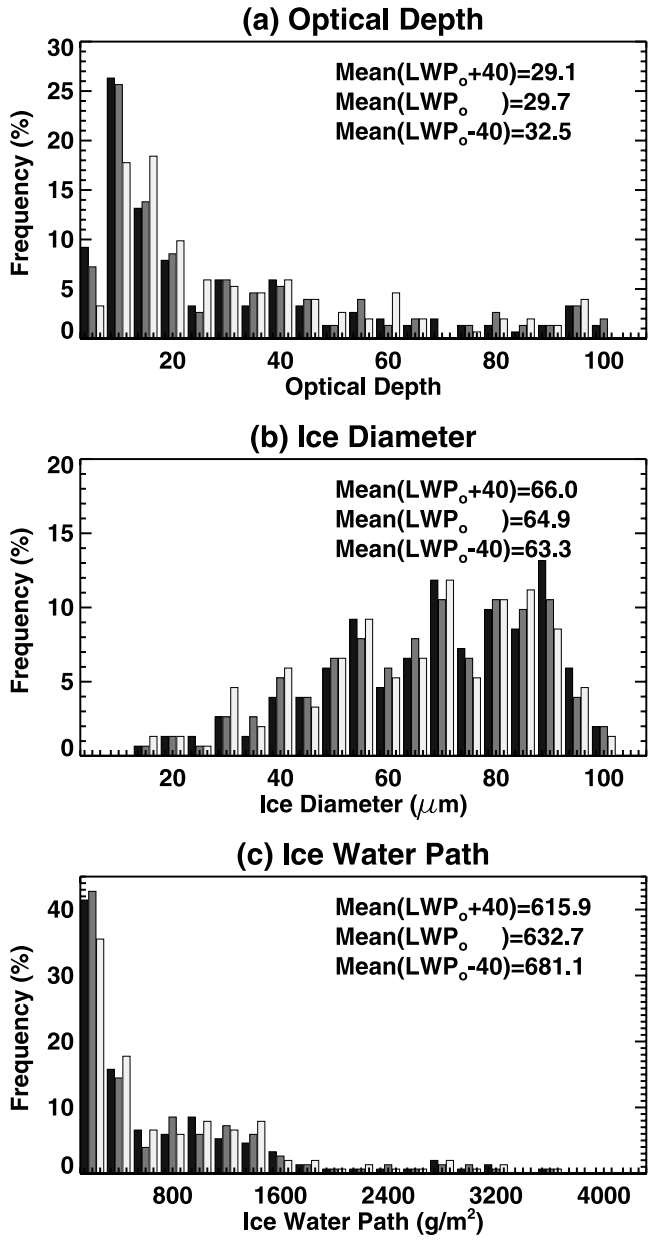

Figure 13. MCRS sensitivity to error in microwave LWP for ice-over-water cloud over four ARM SGP sites (March–October 2000): LWP (+40 gm^{-2}) (black bar), LWP (+0 gm^{-2}) (gray bar), and LWP (−40 gm^{-2}) (light gray bar).

method will be extremely valuable for climate research by providing more accurate retrievals of ice water path than previously possible. The limitation of MCRS is that the algorithm only works in nonprecipitating conditions. It requires ice effective particle sizes less than ~200 μm for satellite remote sensing (such as SSM/I and TMI). For the ARM MWR, the particle size can be as high as 400 μm due to longer wavelengths of MWR than SSM/I which has 85-GHz channels.

[32] **Acknowledgment.** This research was supported by the Environmental Sciences Division of U.S. Department of Energy through the Interagency Agreements DE-AI02-97ER62341 and DE-AI02-02ER63319 under the ARM program.

References

Ackerman, T., and G. Stokes (2003), The Atmospheric Radiation Measurement Program, *Phys. Today*, *56*, 38–45.

Arduini, R. F., P. Minnis, and D. F. Young (2002), Investigation of a visible reflectance parameterization for determining cloud properties in multilayered clouds, in *Proceedings of the 11th AMS Conference on Cloud Physics* [CD-ROM], Am. Meteorol. Soc., Boston, Mass.

Benjamin, S. G., et al. (2004), An hourly assimilation-forecast cycle: The RUC, *Mon. Weather Rev.*, *132*, 495–518.

Cess, R. D., et al. (1990), Intercomparison and interpretation of climate feedback processes in 19 atmospheric general circulation models, *J. Geophys. Res.*, *95*, 16,601–16,615.

Clothiaux, E. E., T. P. Ackerman, G. G. Mace, K. P. Moran, R. T. Marchand, M. Miller, and B. E. Martner (2000), Objective determination of cloud heights and radar reflectivities using a combination of active remote sensors at the ARM CART sites, *J. Appl., Meteorol.*, *39*, 645–665.

Dong, X., P. Minnis, T. P. Ackerman, E. E. Clothiaux, G. G. Mace, R. N. Long, and J. C. Liljegren (2000), A 25-month database of stratus cloud properties generated from ground-based measurements at the ARM SGP site, *J. Geophys. Res.*, *105*, 4529–4537.

Ho, S., B. Lin, P. Minnis, and T. Fan (2003), Estimates of cloud vertical structure and water amount over tropical oceans using VIRS and TMI data, *J. Geophys. Res.*, *108*(D14), 4419, doi:10.1029/2002JD003298.

Huang, J. P., M. M. Khaiyer, P. W. Heck, P. Minnis, and B. Lin (2003), Determination of ice-water path over the ARM SGP using combined surface and satellite data sets, paper presented at 13th ARM Science Team Meeting, Atmos. Radiat. Measure. Prog., U.S. Dept. of Energy, Broomfield, Colo., 31 March to 4 April.

Liljegren, J. C. (1999), Automatic self-calibration of ARM microwave radiometers, in *Microwave Radiometry and Remote Sensing of the Earth's Surface and Atmosphere*, edited by P. Pampaloni and S. Paloscia, pp. 433–443, VSP Press, Utrecht, Netherlands.

Lin, B., and W. B. Rossow (1996), Seasonal variation of liquid and ice water path in non-precipitating clouds over oceans, *J. Clim.*, *9*, 2890–2902.

Lin, B., P. Minnis, B. Wielicki, D. R. Doelling, R. Palikonda, D. F. Young, and T. Uttal (1998), Estimation of water cloud properties from satellite microwave, infrared and visible measurements in oceanic environments: 2. Results, *J. Geophys. Res.*, *103*, 3887–3905.

Lin, B., P. Minnis, A. Fan, J. A. Curry, and H. Gerber (2001), Comparison of cloud liquid water paths derived from in situ and microwave radiometer data taken during the SHEBA/FIREACE, *Geophys. Res. Lett.*, *28*, 975–978.

Liu, G., and J. A. Curry (1998), Remote sensing of ice water characteristics in tropical clouds using aircraft microwave data, *J. Appl. Meteorol.*, *37*, 337–355.

Liu, G., and J. A. Curry (1999), Tropical ice water amount and its relations to other atmospheric hydrological parameters as inferred from satellite data, *J. Appl. Meteorol.*, *38*, 1182–1194.

Mace, G. G., A. J. Heymsfield, and M. R. Poellot (2002), On retrieving the microphysical properties of cirrus clouds using the moments of the millimeter-wavelength Doppler spectrum, *J. Geophys. Res.*, *107*(D24), 4815, doi:10.1029/2001JD001308.

Mace, G. G., Y. Zhang, S. Platnick, M. D. King, P. Minnis, and P. Yang (2005), Evaluation of cirrus cloud properties from MODIS radiances using cloud properties derived from ground-based data collected at the ARM SGP site, *J. Appl. Meteorol.*, in press.

Minnis, P., Y. Takano, and K.-N. Liou (1993), Inference of cirrus cloud properties using satellite-observed visible and infrared radiances, part I: Parameterization of radiance fields, *J. Atmos. Sci.*, *50*, 1279–1304.

Minnis, P., D. F. Young, D. P. Kratz, J. A. Coakley Jr., M. D. King, D. P. Garber, P. W. Heck, S. Mayor, and R. F. Arduini (1995), Cloud optical property retrieval (subsystem 4.3), in *Clouds and the Earth's Radiant Energy System (CERES) Algorithm Theoretical Basis Document*, vol. 3, *Cloud Optical Property Retrieval (Subsystem 4.3)*, *Rep. NASA RP 1376*, edited by CERES Science Team, pp. 135–176, NASA Langley Res. Cent., Hampton, Va.

Minnis, P., D. P. Garber, D. F. Young, R. F. Arduini, and Y. Takano (1998), Parameterization of reflectance and effective emittance for satellite remote sensing of cloud properties, *J. Atmos. Sci.*, *55*, 3313–3339.

Minnis, P., W. L. Smith Jr, D. F. Young, L. Nguyen, A. D. Rapp, P. W. Heck, S. Sun-Mack, Q. Trepte, and Y. Chen (2001), A near-real time method for deriving cloud and radiation properties from satellites for weather and climate studies, in *Proceedings AMS 11th Conference on Satellite Meteorology and Oceanography*, pp. 477–480, Am. Meteorol. Soc., Boston, Mass.

Minnis, P., L. Nguyen, D. R. Doelling, D. F. Young, W. F. Miller, and D. P. Kratz (2002), Rapid calibration of operational and research meteorological satellite imagers, part I: Evaluation of research satellite visible channels as references, *J. Atmos. Oceanic Technol.*, *19*, 1233–1249.

Weng, F., and N. C. Grody (2000), Retrieval of ice cloud parameters using a microwave imaging radiometer, *J. Atmos. Sci.*, *57*, 1069–1081.

Zhao, L., and F. Weng (2002), Retrieval of ice cloud parameters using the advanced microwave sounding unit, *J. Appl. Meteorol.*, *41*, 384–395.

R. F. Arduini and A. Fan, SAIC, One Enterprise Parkway, Suite 300, Hampton, VA 23666, USA.

J. Huang, M. M. Khaiyer, and Y. Yi, Analytical Services and Materials, One Enterprise Parkway, Suite 300, Hampton, VA 23666, USA. (j.huang@larc.nasa.gov)

B. Lin and P. Minnis, Mail Stop 420, NASA Langley Research Center, Hampton, VA 23681, USA.

G. G. Mace, Department of Meteorology, University of Utah, Salt Lake City, UT 84112, USA.